Within-individual leaf trait variation increases with phenotypic integration in a subtropical tree diversity experiment

Pablo Castro Sánchez-Bermejo[1,2] (iD), Andréa Davrinche[1,2,3] (iD), Silvia Matesanz[4] (iD), W. Stanley Harpole[1,2,5] (iD) and Sylvia Haider[1,2,6] (iD)

[1]Institute of Biology/Geobotany and Botanical Garden, Martin Luther University Halle-Wittenberg, Halle (Saale), 06108, Germany; [2]German Centre for Integrative Biodiversity Research (iDiv) Halle-Jena-Leipzig, Puschstraße 4, Leipzig, 04103, Germany; [3]Research Centre for Ecological Change (REC), Organismal and Evolutionary Biology Research Programme, Faculty of Biological and Environmental Sciences, University of Helsinki, Helsinki, 00014, Finland; [4]Área de Biodiversidad y Conservación, Departamento de Biología, Geología, Física y Química inorgánica, ESCET, Universidad Rey Juan Carlos, Móstoles, 28933, Spain; [5]Department of Physiological Diversity, Helmholtz Centre for Environmental Research – UFZ, Leipzig, 04103, Germany; [6]Leuphana University of Lüneburg, Institute of Ecology, Lüneburg, 21335, Germany

Author for correspondence:
Pablo Castro Sánchez-Bermejo
Email: pablo.castro@idiv.de

Summary

- Covariation of plant functional traits, that is, phenotypic integration, might constrain their variability. This was observed for inter- and intraspecific variation, but there is no evidence of a relationship between phenotypic integration and the functional variation within single plants (within-individual trait variation; WTV), which could be key to understand the extent of WTV in contexts like plant–plant interactions.

- We studied the relationship between WTV and phenotypic integration in *c.* 500 trees of 21 species in planted forest patches varying in species richness in subtropical China. Using visible and near-infrared spectroscopy (Vis-NIRS), we measured nine leaf morphological and chemical traits. For each tree, we assessed metrics of single and multitrait variation to assess WTV, and we used plant trait network properties based on trait correlations to quantify phenotypic integration.

- Against expectations, strong phenotypic integration within a tree led to greater variation across leaves. Not only this was true for single traits, but also the dispersion in a tree's multitrait hypervolume was positively associated with tree's phenotypic integration. Surprisingly, we only detected weak influence of the surrounding tree-species diversity on these relationships.

- Our study suggests that integrated phenotypes allow the variability of leaf phenotypes within the organism and supports that phenotypic integration prevents maladaptive variation.

Introduction

Trait-based plant ecology assumes that plant attributes, that is, functional traits, mediate community assembly and ecosystem processes (Violle *et al.*, 2007; Shipley *et al.*, 2016). Traditionally, this discipline focused on mean differences between species' traits (i.e. interspecific trait variation) to address ecological questions related, for example, to plant coexistence or niche differentiation, ignoring that trait variation may also occur within species (i.e. intraspecific variation; Bolnick *et al.*, 2011; Violle *et al.*, 2012). However, by only considering interspecific trait variation we might fail to explain ecosystem processes at the spatial scales where individuals interact and, indeed, it is agreed that ignoring variability within species can lead to biased conclusions (Bolnick *et al.*, 2011; de Bello *et al.*, 2011; Chase, 2014). Recently, there has been a growing effort to understand the role of variation at lower levels of biological organization (Escudero & Valladares, 2016; Hart *et al.*, 2016; Escudero *et al.*, 2021). While variation

among individuals within a species (i.e. intraspecific trait variation) has gained attention (Hart *et al.*, 2016; Des Roches *et al.*, 2018), only few studies addressed the ecological role of within-individual trait variation (WTV; see Table 1). Within-individual trait variation (WTV) refers to the plastic responses of plant individuals to express different trait values across different repeated architectural units of the plant body structure (De Kroon *et al.*, 2005; Herrera *et al.*, 2015; Herrera, 2017). Far from being 'phenotypic noise', plants show within-individual responses in, for example, leaf (Winn, 1996; Valladares & Niinemets, 2008; Møller *et al.*, 2022), fruit (Sobral *et al.*, 2019) or flower traits (March-Salas *et al.*, 2021). Furthermore, this variation may affect plant performance (Herrera, 2009, 2017) and can have evolutionary consequences (Herrera *et al.*, 2022; Sobral & Sampedro, 2022).

The variation of one trait is not necessarily independent from the variation of other traits. Indeed, there are numerous and complex trait relationships resulting from genetic, developmental,

Table 1 Definition of acronyms and abbreviations used.

Acronym/abbreviation	Definition
WTV	Within-individual trait variation
PI_{ind}	Individual phenotypic integration
BEF	Biodiversity–ecosystem functioning
Vis-NIRS	Visible and near-infrared spectrometry
SLA	Specific leaf area
LDMC	Leaf dry matter content
C : N	Carbon-to-nitrogen ratio
C	Carbon leaf content
N	Nitrogen leaf content
Mg	Magnesium leaf content
K	Potassium leaf content
Ca	Calcium leaf content
P	Phosphorous leaf content
FRic	Functional richness
FDis	Functional dispersion
SD	Standard deviation
LMM	Linear mixed model
AIC	Akaike information criterion

and/or functional trade-offs and allometric constraints (Gould & Lewontin, 1979; Wright *et al.*, 2004; Huneman, 2010; Armbruster *et al.*, 2014; Nielsen & Papaj, 2022). For example, a reduction in specific leaf area (SLA) is usually coupled with an increase in leaf dry matter content (LDMC; Wright *et al.*, 2004). Under this premise, traits vary in a coordinated way to optimize some functions at the cost of others (Messier *et al.*, 2017; Vasseur *et al.*, 2022). As a result, it is suggested that phenotypic integration (i.e. the pattern of coordination and covariation among traits reflected by the amount of significant correlations between traits, Schlichting & Pigliucci, 1998; Gianoli & Palacio-López, 2009; Armbruster *et al.*, 2014) could play a role in constraining trait variation (Valladares *et al.*, 2007; Matesanz *et al.*, 2021). This assumption is also based on the impossibility of the evolution of organisms that can reach an optimal value for every trait simultaneously (Rees, 1993; Laughlin & Messier, 2015). That is why under scenarios of strong phenotypic integration, only a subset of possible trait combinations will exist due to the presence of strong constraints from functional trade-offs (Laughlin *et al.*, 2017). Thus, different levels of phenotypic integration may be associated with the expression of plastic responses (He *et al.*, 2021; Homeier *et al.*, 2021; Silva *et al.*, 2021; Li *et al.*, 2022; Xie & Wang, 2022). However, while previous evidence describing the relationship between phenotypic integration and trait variation stems from studies on interspecific and intraspecific trait variation, the relationship between plant individuals' phenotypic integration (PI_{ind}; i.e. the number of significant correlations among traits between different repeated units of the same individual) and WTV is not known (but see Escribano-Rocafort *et al.*, 2017). Therefore, understanding this relationship is crucial to assess the extent and intrinsic limits of WTV in modular organisms. To our knowledge, the only study focusing on PI_{ind} and WTV simultaneously suggested that for olive trees (*Olea europaea*) with higher leaf PI_{ind}, leaf WTV tended to be lower (Escribano-Rocafort *et al.*, 2017). According to these results, and similarly to what has

been found at higher levels of biological organization (He *et al.*, 2021), differences in PI_{ind} among individuals might explain differences in WTV. It could be therefore expected that individuals with higher PI_{ind} would be limited in their WTV. Therefore, phenotypic integration could affect the amount of WTV as a response to abiotic and biotic drivers.

Resource competition is considered a major component of plant–plant interactions. In theory, each individual inhabits a particular niche where it competes for resources with its local neighbors (Cabal *et al.*, 2021). Accordingly, it is well established that there are stabilizing mechanisms that support species coexistence through functional differentiation and niche complementarity (Wright *et al.*, 2014). Also, within species, niche complementarity between individuals of the same population can diminish the strength of intraspecific competition, since individuals from the same species need common resources and share similar uptake pathways (Grime, 1973; Tilman *et al.*, 1982). Such niche complementarity through trait variation within species is particularly important in communities with low taxonomic diversity and, hence, high levels of intraspecific competition (Gross *et al.*, 2008; Götzenberger *et al.*, 2012). In this context, as WTV may improve efficiency in the use of resources (Møller *et al.*, 2022), it has been suggested as a mechanism to foster niche complementarity and reduce intraspecific competition for resources among plants interacting directly (Davrinche *et al.*, 2023). Indeed, WTV was reported to decrease with taxonomic diversity of the local neighborhood (Proß *et al.*, 2021). However, as WTV is expected to be limited by phenotypic integration (Escribano-Rocafort *et al.*, 2017), this could cause plants to fail to produce the optimal suites of traits for a given microenvironment (Pigliucci, 2005). Therefore, understanding the effect of neighborhood diversity on WTV and on the WTV-PI_{ind} relationship remains crucial to assess the role and intrinsic limits of trait variation in plant–plant interactions.

Leaves are repeated organs within plants with a crucial role in resource acquisition via photosynthesis. Furthermore, the light interception by leaves is a key factor in competition (Valladares *et al.*, 2016). That is why plants express different leaf phenotypes within the crown in order to adjust to the light exposure (Sack *et al.*, 2006; Escribano-Rocafort *et al.*, 2016; Mediavilla *et al.*, 2019). In addition, plastic responses in leaf traits are specifically noticeable in trees, which have great potential to express WTV as a consequence of their high modularity (Watkinson & White, 1986) and, therefore, could provide a suitable model to study the relationship between trait variation and phenotypic integration within an individual. As light heterogeneity is influenced, among others, by the canopy structure of the community, trees are expected to adjust their leaves to the different light exposures generated by different levels of taxonomic diversity. Consequently, a tree's leaf WTV may be strongly affected not only by the taxonomic identity of the closest tree neighbor but also by the taxonomic diversity of the surrounding tree neighborhood (Proß *et al.*, 2021).

Here, we studied patterns of leaf trait variation and phenotypic integration within individual trees and how they were affected by local taxonomic diversity. As the closest adjacent tree is expected

to have the strongest effect on intraspecific trait variation (Davrinche & Haider, 2021), we considered two scales of local taxonomic diversity: taxonomic diversity of the local neighborhood, that is, the trees surrounding a focal individual in a community, and identity of the closest neighbor. We used the currently largest tree diversity experiment, located in subtropical China, and measured nine morphological and chemical leaf traits in *c.* 500 individuals from 21 species across plots differing in species composition. We assessed different metrics of functional trait variation (WTV) and phenotypic integration for each individual tree. We expected that higher PI_{ind} constraints WTV (Fig. 1). As higher WTV is expected for scenarios of high intraspecific competition, we also expected that the WTV-PI_{ind} relationship depends on taxonomic diversity. Specifically, we hypothesized that the constraint should be more pronounced in scenarios of high taxonomic diversity (i.e. in diverse communities and, especially, when trees are directly interacting with a heterospecific adjacent neighbor) due to the lower ecological relevance of WTV in these environments (Fig. 1). Contrary, in scenarios of low taxonomic diversity, trees are expected to prioritize the display of alternative leaf designs, even if integration is high. We expected

the constrain of PI_{ind} on WTV for the WTV of individual traits and also for metrics of multitrait functional diversity.

Materials and Methods

Study site

This study was conducted in a biodiversity–ecosystem functioning (BEF) experiment, the BEF-China tree diversity experiment, located in Xingangshan, in Jiangxi Province (lat. 29°08′11″N, long. 117°90′93″E; Fig. 2a). BEF-China was designed to study ecosystem functions in planted patches of varying tree-species richness, hence simulating the effect of species extinction on the functioning of ecosystems. The climate is subtropical with a mean annual temperature of 16.5°C (ranging from 0.4°C in January to 34.2°C in July) and mean annual precipitation of 1821 mm (data from the adjacent Wuyuan County, Yang *et al.* (2013)). The natural vegetation in the region is dominated by mixed broadleaved forests with similar number of deciduous and evergreen species, but with evergreen species dominating in terms of abundance (Bruelheide *et al.*, 2011; Su *et al.*, 2020).
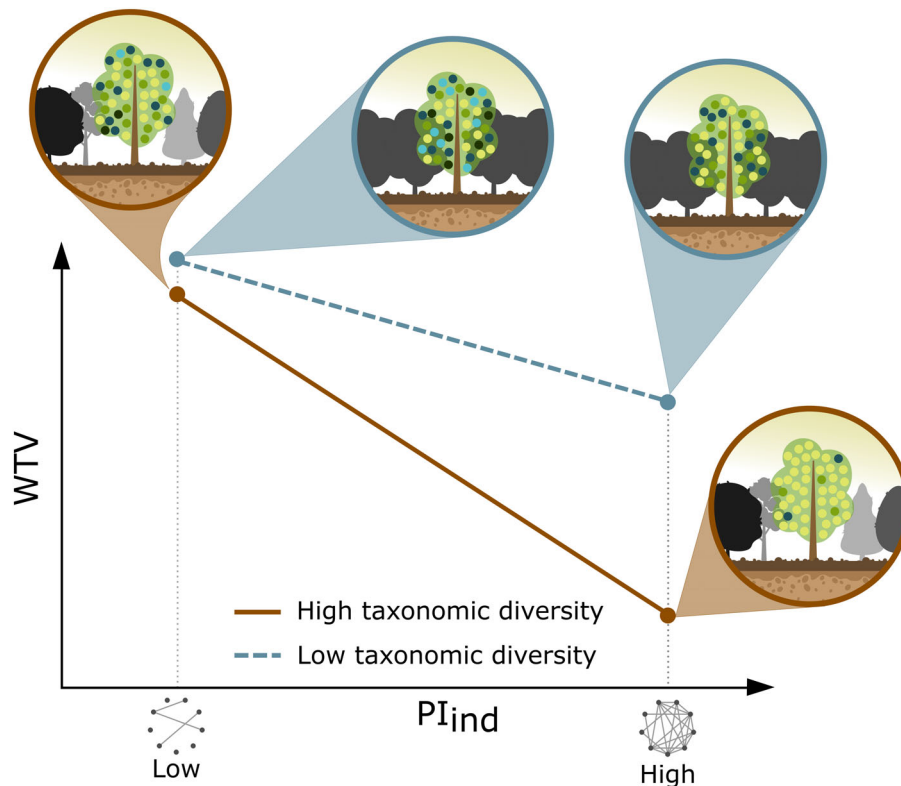

Fig. 1 Expected relationship between individual phenotypic integration (PI_{ind}) and within-individual trait variation (WTV) at different levels of tree diversity. PI_{ind} is expected to constrain WTV at both levels of taxonomic diversity (Hypothesis 1), indicated in the figure through color variation in leaves. However, as WTV is an important mechanism to drive niche differentiation as response to intraspecific competition, we expect the WTV-PI_{ind} relationship to depend on the local taxonomic diversity, including both the identity of the adjacent neighbor and the diversity of species in the neighborhood (Hypothesis 2). Thus, the constraint of WTV by PI_{ind} should be less pronounced in scenarios of low taxonomic diversity. Networks on the bottom of the x-axis represent two scenarios of PI_{ind}, where lines ('edges') connecting points indicate coordination between two traits. Thus, low PI_{ind} (left) occurs when the number of coordinated pair of traits is low, while high PI_{ind} (right) indicates that the number of coordinated pair of traits is high. Zoom areas show the leaf WTV of a target tree (denoted by variable colored points within the crown) in different contexts of taxonomic diversity (represented by the shape and transparency of the tree silhouettes surrounding the target tree).
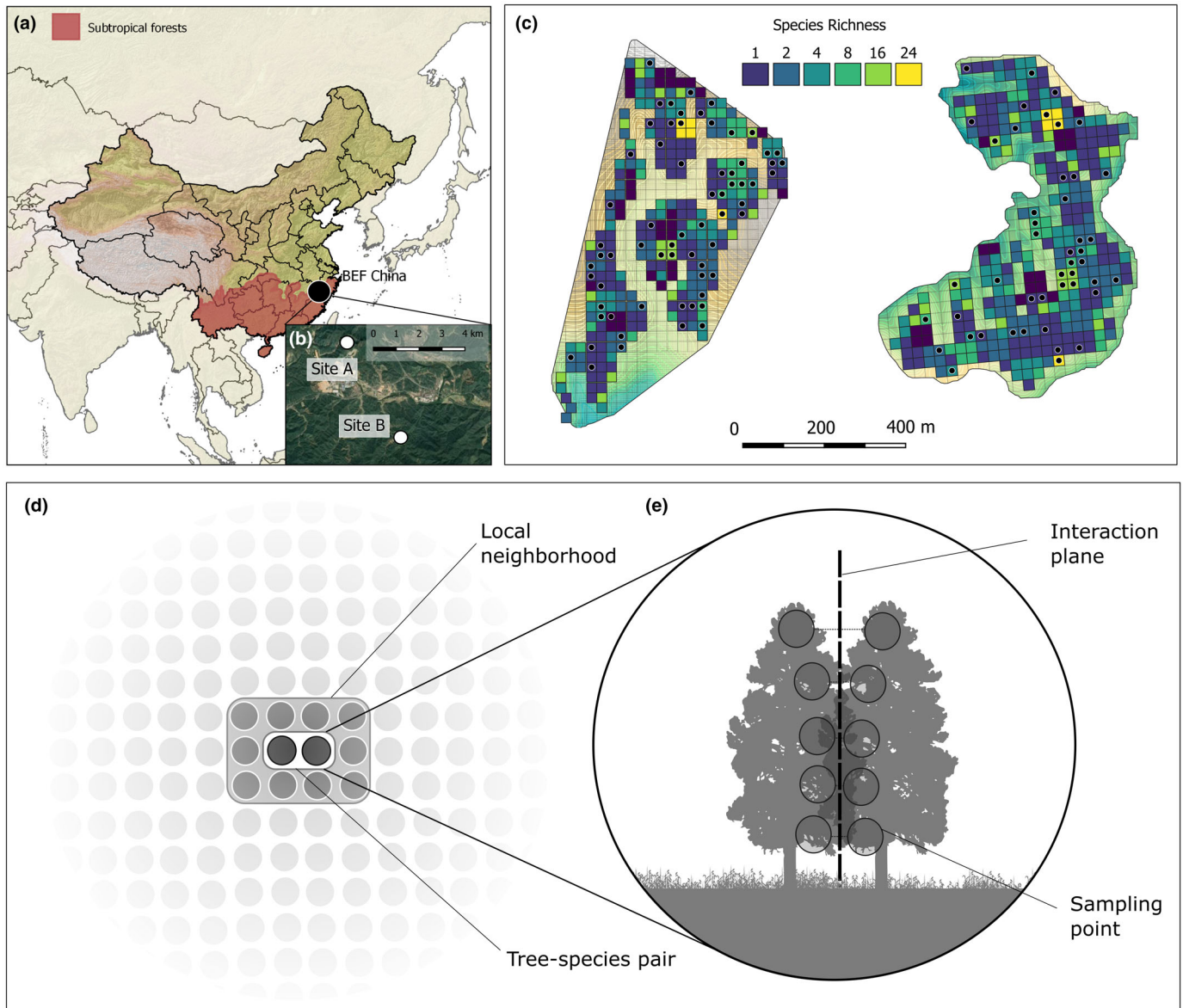
Fig. 2 Location of (a) the biodiversity–ecosystem functioning (BEF)-China experiment, (b) sites of the experiment and (c) plots within the sites, and (d, e) design of the tree-species pair sampling. The BEF-China experiment (a) is located in subtropical China (Xingangshan, Jiangxi Province). The map also shows in addition the distribution of subtropical forests in China (Olson *et al.*, 2001). The experiment consists (b) of two sites (A and B) distanced by *c*. 5 km. Each site contains plots differing in the number of planted species (c). The black dots in (c) indicate the plots where sampling took place for this study. As shown in (d), within plots we selected at least one tree-species pair, consisting of two adjacent trees directly interacting, and defined the local neighborhood of a tree-species pair as the group of 10 trees that were directly surrounding the tree-species pair. For every tree-species pair, we sampled leaves at five different heights (sampling points) along the vertical plane between the trees (interaction plane), which is represented by the dashed line (e).

The experiment consists of two sites, A and B, where trees were planted in 2009 and 2010, respectively (Bruelheide *et al.*, 2014; Fig. 2b). Site A extends over an area of 27 ha with an elevation ranging from 205 to 275 m asl and slopes from 8.5° to 40°. Site B has a size of > 23 ha with an elevation ranging from 113 to 182 m asl and slopes ranging from 15° to 43°. In the experiment, trees are arranged following the 'broken-stick' design described in Bruelheide *et al.* (2014). This design is based on the partitioning of the pool of species in every site into two equal groups at each subordinate richness level. Thus, from the total pool of 40 species in both sites (see Bruelheide *et al.* (2014) for details on the plant

species), plots range from the 24-species mixture to the monoculture passing through 16-, 8-, 4- and 2-species mixtures (Fig. 2c). Hence, at each site, all species are equally represented at every species richness level. In every plot, 400 saplings from local nurseries were planted in a regular grid with a distance of 1.29 m, with species randomly assigned to planting positions.

Field sampling

Sampling followed the tree-species pair design as described in Trogisch *et al.* (2021), which focuses on the interaction of a pair

of directly adjacent neighbors (hereafter, referenced as tree-species pair) and the interaction of this tree-species pair with the surrounding local neighborhood (Fig. 2d). Hence, by sampling both trees in a tree-species pair, the design allows to study the interaction between WTV and individual phenotypic integration (PI_{ind}) at two different fine scales of local taxonomic diversity: the species identity of the tree-species pair partner, that is, the tree's closest neighbor (conspecific vs heterospecific); and the taxonomic diversity of the local neighborhood, that is, the 10 trees (or fewer in case of mortality) surrounding the tree-species pair. The diversity of the local neighborhood was assessed by calculating the Shannon index (Shannon, 1948), considering the frequency of the different tree species within the up to 10 neighbor trees of the tree-species pair.

Sampling took place from late August to early October 2018 and mid-August to mid-September 2019 for sites A and B, respectively. We sampled a total of 432 trees (216 tree-species pairs) in 69 plots at site A and 437 trees (219 tree-species pairs) in 57 plots at site B (hereafter, referenced as regular set). From each tree, we collected leaves along the interaction plane between the tree-species pair partners (the vertical plane where the two crowns of the tree-species pair partners meet, Fig. 2e). In order to encompass the variation of the whole individual, we sampled at five different heights along the interaction plane. At each height, we cut three fully developed leaves free from mechanical or pathogen damage. Immediately after collection, leaves were stored in sealable plastic bags with moistened tissue. Samples were transported in an isothermal bag equipped with cooling bags to prevent dehydration. In the laboratory, samples were temporarily stored at 6–8°C.

In addition, we collected an independent set of leaf samples for each site (hereafter, referenced as calibration sets). The aim of this was to predict the trait values for the samples of the regular set based on the relationship between reflectance spectra and measured trait values of the calibration set. For the calibration sets, we aimed to include 10 leaf samples per species per site across all plots of all species richness levels, collected at different heights and orientation within the crown, in order to maximize the sampled scenarios (i.e. combinations of species considering the closest neighbor and the local neighborhood, different position of the leaf within the crown and location of the tree within the experimental site). A total of 236 samples for site A and 252 for site B were collected for the calibration set, with each sample composed of 15 leaves on average depending on the leaf size, to ensure sufficient material for laboratory analyses.

Laboratory analyses

The number of leaf samples in the regular set was high, and the material from each leaf was too low to conduct all chemical analyses at the leaf level. For this reason, we used visible and near-infrared spectrometry (Vis-NIRS), a technique of massive phenotyping, to estimate trait values for each individual leaf based on calibration models (Foley et al., 1998; Escudero et al., 2021). For all leaves (regular and calibration sets), we acquired reflectance spectra with a portable Vis-NIRS device (ASD

'FieldSpec4' Wide-Res Field Spectroradiometer; Malvern Panalytical Ltd, Almelo, the Netherlands). Reflectance was measured across the full range of solar radiation spectrum (250–2500 nm), by taking three repeated measurements on the adaxial side of each leaf while avoiding main veins. For each of these repeated measurements, 10 spectra were averaged internally to reduce noise. The equipment was optimized regularly with a calibration white panel (Spectralon, Labsphere, Durham, NH, USA).

For the samples of the calibration set, we determined nine morphological and chemical leaf traits which are assumed to reflect a plant's strategy in terms of the investment of nutrients and dry mass in the leaves (Pérez-Harguindeguy et al., 2013; Díaz et al., 2016; see Supporting Information Table S1). Additionally, these traits are key components of the leaf economics spectrum and reflect the most important trade-offs along different leaf designs (Wright et al., 2004; Osnas et al., 2013): specific leaf area (SLA; leaf area divided by leaf dry mass), leaf dry matter content (LDMC; leaf dry mass divided leaf fresh mass), carbon-to-nitrogen ratio (C : N), carbon content (C), nitrogen content (N), magnesium content (Mg), potassium content (K), calcium content (Ca), and phosphorus content (P). After collection, the saturated fresh leaves of the calibration samples were weighed (DeltaRange Precision Balance PB303-S; Mettler-Toledo GmbH, Gießen, Germany) and scanned at a resolution of 300 dpi to calculate leaf area (WinFOLIA; Regent Instruments, Quebec, QC, Canada). Leaves were oven-dried at 80°C for 72 h and weighed to calculate SLA and LDMC. Dried leaves were ground (Mixer Mill 400; Retsch, Haan, Germany), and 200 mg of the resulting powder was used for a nitric acid digestion. After the digestion, Mg, Ca, and K were analyzed with atomic absorption spectrometry (ContrAA 300 AAS; Analytik Jena, Jena, Germany), while P was measured through a molybdate spectrophotometric method. Additionally, we used an elemental analyzer (Vario El Cube; Elementar, Langenselbold, Germany) to gas-chromatographically determine C and N and, from these measurements, C : N.

Leaf spectra of the samples of the calibration set were analyzed with the UNSCRAMBLER X software (v.10.1; CAMO Analytics, Oslo, Norway) for all species together but separately for site A and site B. The use of multispecies calibrations aimed to cover the broadest trait space possible, in order to better reflect the possible variation in our samples (Burnett et al., 2021) and allowed for more data to build the calibration model. Spectral pretreatments were applied in order to optimize the prediction of traits (normalization, smoothing and 2nd derivate, orthogonal signal correction, standard normal variate, detrending according to Barnes et al. (1989), or baseline correction). Spectra were then used to fit partial least square regression models by using the NIPALS algorithm (Dayal & Macgregor, 1997; Burnett et al., 2021). Selection of the partial least square regression models was based on their quality (determined by a high R^2 value and a low root mean square error for a validation set), parsimony (indicated by a low number of factors), and predictive power (determined by a high R^2 for predicted vs reference value). For site A, R^2 for predicted vs reference value of the best models for each trait was 66.94 ± 20.23 (mean $\pm$ standard deviation), with a maximum R^2

for SLA (88.90) and minimum for Ca (24.20), while for site B we obtained a mean R^2 of 74.60 ± 11.00, with maximum and minimum values for SLA (89.88) and Ca (58.84), respectively (see Davrinche & Haider (2021) and Davrinche *et al.* (2023) for methodical details). Finally, these models were used to predict the trait values from the reflectance spectra of the samples of the regular set. From the three predicted values for each leaf in the regular set (resulting from the three repeated measurements per scan), we excluded: negative ones; those with > 5% deviation from the range limits of the calibration data; and values outside of the 95% confidence interval of the model prediction. The remaining values per leaf were averaged. As a consequence of outlier detection, an average of 3.3 ± 1.1% (mean ± SD) of the leaves was removed depending on the trait (see Table S2).

Metrics of individual phenotypic integration and trait variation

To accurately estimate PI_{ind} and WTV, we only used data from those trees, which met several criteria in the regular dataset. Thus, as the study of phenotypic integration requires the lack of missing data (He *et al.*, 2020) only leaves with trait data available for all nine traits were considered. Furthermore, in order to avoid low accuracy in the metrics for WTV, and especially, for PI_{ind}, only trees with data from a minimum of 10 leaves were considered (see Fig. S1 for details on data selection). Finally, as the underrepresentation of specific sampled species could make sample sizes across groups highly unbalanced and, thus, our models unstable (Grueber *et al.*, 2011), we only worked with those species which after the filtering described before were represented by more than eight individuals. Thus, from the original number of 869 trees from 27 species, our study included 499 trees from 21 species located in 97 plots and represented across different levels of taxonomic diversity (see Tables S3, S4).

To measure PI_{ind}, we first computed for each tree all possible pairwise correlations between traits based on the trait values for individual leaves (Fig. S2a). Then, we evaluated the significance of the correlations by using permutation tests in which trait values were rearranged 20 000 times and pairwise correlations were calculated from each randomization. We calculated the *P*-values based on the permutation distribution of correlations obtained from randomizations. These tests were performed by using the function perm.cor.test in the JMUOUTLIER package (Garrenstjmuedu, 2019). Based on our correlation matrix, we built a plant trait network for each tree as described in He *et al.* (2020). To avoid spurious correlations among traits, we only considered connections ('edges') of significant correlation ($P < 0.05$) and with a Pearson coefficient $|\rho| \geq 0.6$ (Aggarwal & Ranganathan, 2016). Importantly, most trait–trait pairs considered for the network were highly significant ($P < 0.01$), indicating that the considered correlations are not likely statistical noise but, rather, a biological signal (see Figs S3, S4). We measured two properties that estimate the tightness of the networks: edge density, which measures the proportion of actual connections among traits out of all possible connections within a network and, thus, can be used to quantify the connectivity of all traits

across the whole trait network (Benavides *et al.*, 2021); and degree (Poorter *et al.*, 2014; He *et al.*, 2021), which represents a measure of coordination for each trait as it measures the number of connections of one focal trait ('node') to all others. These properties of the networks were assessed by using functions from the IGRAPH package (Csardi, 2021).

We assessed multitrait WTV for each tree including all traits by using two indices related to different attributes of the functional hypervolume of all leaves in a tree: functional richness (FRic); and functional dispersion (FDis). Together, these two indices can reveal two different and complementary aspects of trait variation. Functional richness (FRic) measures the total functional hypervolume by using the minimum convex volume (Cornwell *et al.*, 2006; Botta-Dukát & Czúcz, 2016). This index aims to detect reductions in the niche space occupied by individuals (Cornwell *et al.*, 2006). Thus, a higher FRic indicates that an individual occupies a greater niche space. Functional dispersion (FDis) measures the distances of leaves to the centroid of the functional hypervolume, thus describing whether the distribution of leaves in a trait space is clustered or dispersed (Laliberte & Legendre, 2010). To calculate these indices, we first obtained a leaf-by-leaf trait distance matrix per tree by using Gower's distance. This was calculated with the gowdis function in the FD package (Laliberté *et al.*, 2014). Then, for every tree we computed both indices through principal coordinate analysis (PCoA) by using the function dbFD from the same package. As these indices can be sensitive to the number of observations and in order to account for the different number of leaves per tree (Mason *et al.*, 2013), we used standardized effect sizes (SES) as described in Gotelli & McCabe (2002). We used 500 randomizations in a null-model analysis to ensure accurate estimates of SES values. Additionally, we assessed single-trait WTV by using the standard deviation (SD) of each trait across all leaves within a tree, as it represents how trait values are spread around the mean value (Proß *et al.*, 2021; Fig. S2b).

Statistical analyses

All statistical analyses were performed in R v.4.02 (R Core Team, 2021). To assess the joint effect of PI_{ind} and local taxonomic diversity on within-tree trait variation (WTV), we performed linear mixed models (LMMs) for the multitrait and single-trait metrics of WTV. To do so, we used the two functional indices (SES(FDis) and SES(FRic)) and the SD of each of the nine traits, respectively, as response variables, resulting in a total of 11 models. Explanatory variables were the two metrics for PI_{ind} (edge density in the case of multitrait WTV (SES(FDis) and SES(FRic)), and the degree in the case of the models for single-trait WTV (SD)), the diversity of the tree-species pair (conspecific vs heterospecific), the Shannon diversity of the local neighborhood of a tree-species pair, and all possible interactions of these variables (including the three-way interaction). We included tree-species pair identity nested in plot, in turn nested in site, and species identity as crossed random effects in order to account for the design of the experiment and differences among species, respectively (see Table S5). These analyses were

conducted using the lmer function in the LMERTEST package (Kuznetsova *et al.*, 2017). We used diagnostic plots of the residuals to study the assumptions of normality, homoscedasticity and linearity in our models: residuals vs fitted values plots, histograms of the residuals and Q-Q plots for the deviance of the residuals. Thus, to meet the premises of homoscedasticity and normality of the residuals in the models, SD(SLA), SD(C), and SD(P) were log-transformed and SD(LDMC), SD(N), SD(K), and SD(Ca) were square-root transformed. We fitted 'beyond optimal' models, which included all of the fixed effects to fit the model. Then, by including only subsets of the predictors, the AIC was calculated for all possible models that varied in their fixed effects. We selected all models with ΔAIC lower than 2 as competing models holding similar information and followed the principle of parsimony to prioritize the simplest model with the smallest number of predictors among all competing models (Burnham & Anderson, 2004; Richards *et al.*, 2011; Harrison *et al.*, 2018). Finally, we assessed the quality of fit of our competing models by calculating the marginal and conditional R^2, which address the variance explained only by fixed effects and the variance explained by the entire model, respectively.

Results

We found a positive relationship between multitrait WTV and PI$_{ind}$. However, of the two multitrait functional indices, only SES(FDis) responded to edge density, which was used to quantify PI$_{ind}$ at the multitrait level (Table 2). In both competing models, SES(FDis) increased with edge density and this response was stronger for trees with a conspecific partner (significant interaction of edge density and the diversity of the tree-species pair; Figs 3, 4a). Furthermore, one of the competing models, but not the simplest model, included a negative effect of local neighborhood Shannon diversity, indicating that higher local neighborhood diversity was associated with lower SES(FDis; see Fig. S5). The effect of edge density on SES(FRic) was included in three of the competing models, but the most parsimonious model neither included edge density nor any of the other predictor variables. In the three competing models including edge density among the predictors, two suggested that SES(FRic) increases with edge density while the third indicated that the response depends on the identity of the closest neighbor, increasing in the case of a conspecific partner and decreasing in the case of a heterospecific one (see Fig. S6). This suggests that the effect of edge density on SES(FRic) was rather weak and could be attributable to correlations between metrics (see Fig. S4). For the most parsimonious model of SES(FDis), marginal R^2 accounted for 13% of the variance, and 17% of the variance was explained when also considering the random effects as well. In the case of SES(FRic), for the simplest model, conditional R^2 accounted for 8% of the variance.

In the single-trait analyses, WTV (quantified through trait SD) increased with increasing PI$_{ind}$ (quantified through degree, i.e. the number of significant associations of that trait with others) in all competing models (Table 2; Fig. 4c–k). In contrast, the effect of taxonomic diversity and its role in mediating the response of single-trait WTV to PI$_{ind}$ was not included in all

competing models. Local neighborhood Shannon diversity appeared as a predictor in at least one of the competing models for each trait (see Figs 3, S7–S15), suggesting that Shannon diversity of the local neighborhood may cause a decrease in WTV. However, only in the case of Ca this effect was included in the simplest model (Fig. 5). Similarly, tree-species pair diversity (conspecific vs heterospecific) was maintained as a predictor in at least one competing model for all traits, but never in the simplest model. For all traits, except for Mg and Ca, there was slightly more WTV in trees with conspecific partners. Interactions between PI$_{ind}$ and local neighborhood Shannon diversity were found among some of the competing models for C : N, C, K and Ca, suggesting in most cases that the response of WTV to PI$_{ind}$ could be slightly stronger when local neighborhood diversity decreases. In the case of the interaction between degree and tree-species pair diversity, this effect was present among some of the competing models for SLA, LDMC, N, and K, but the effect of the interaction was inconsistent across traits (see Figs S7, S8, S11, S13). In most cases, marginal R^2 accounted for a small portion of the total variance in the simplest models (varying between *c.* 5% in the case of Mg and P and *c.* 15% for the models of SLA, LDMC, N, and Ca), but conditional R^2 accounted for a greater portion of the variance (varying from *c.* 27% in P to *c.* 85% in P; see Table 2). This suggests that even though we found a correlation between PI$_{ind}$ and WTV, the predictive ability of these models is rather low.

Discussion

By using multiple leaves from each of 499 tree individuals from 21 species in a tree diversity experiment in subtropical China, we assessed whether WTV is influenced by PI$_{ind}$, and how tree-species diversity affects this relationship. Contrary to our expectation, our results showed that high individual WTV was associated with higher PI$_{ind}$. We found this response for FDis, a metric including all traits measured and reflecting the mean distance of each leaf to the centroid in a multidimensional trait space (i.e. how much a tree's leaves differ from the average trait values of all leaves of this tree), and for single traits' SD (i.e. leaves' deviation from the tree's mean considering single traits). To our knowledge, this is the first study showing such a consistent positive relationship between the integration of the phenotype and WTV. In contrast to the consistent response of FDis, the total trait hypervolume estimated by FRic did not show a clear pattern. Referring to the best and simplest model, the positive associations between WTV and PI$_{ind}$ were mediated by taxonomic diversity only in the case of FDis, for which the response was stronger in conspecific tree-species pairs. Furthermore, WTV of leaf Ca showed a decrease in response to local neighborhood Shannon diversity.

In disagreement with our first hypothesis, our results suggest that PI$_{ind}$ and WTV did not follow the same pattern described for higher levels of biological organization (inter- and intraspecific trait variation). The trade-off between trait variation and phenotypic integration is a widely spread statement in ecology (Valladares *et al.*, 2007) and was observed for interspecific trait variation (Dwyer & Laughlin, 2017; He *et al.*, 2021; Silva *et al.*,

Table 2 Competing models to identify the drivers of within-individual trait variation (WTV).

Response	Int	PI_{ind}	S	TSP_{Div}	PI_{ind} : S	PI_{ind} : TSP_{Div}	S : TSP_{Div}	PI_{ind} : S : TSP_{Div}	df	Delta	R^2_m	R^2_c
SES(FDis)	**−3.085**	**1.992**		**−0.824**	×				**9**	**0**	**0.133**	**0.174**
	−3.021	2.002	−0.075	−0.845	×				10	1.471	0.135	0.177
SES(FRic)	−0.493	0.236							7	0	0.005	0.093
	−0.374								**6**	**0.585**	**0**	**0.084**
	−0.339	−0.08		−0.244	×				9	1.48	0.01	0.109
	−0.503	0.24	0.011						8	1.942	0.005	0.1
log(SLA$_{SD}$)	**2.385**	**0.089**							**7**	**0**	**0.062**	**0.709**
	2.374	0.088		0.023					8	1.557	0.062	0.71
	2.401	0.088	−0.019						8	1.671	0.062	0.71
	2.292	0.106		0.15	×				9	1.853	0.063	0.712
sqrt(LDMC$_{SD}$)	**3.889**	**0.242**							**7**	**0**	**0.163**	**0.267**
	3.691	0.238	0.21	0.295			×		10	1.115	0.169	0.272
	3.513	0.278	0.21	0.585		×	×		11	1.401	0.173	0.273
	3.907	0.242	−0.025						8	1.94	0.163	0.268
(C : N)$_{SD}$	**2.069**	**0.299**							**7**	**0**	**0.123**	**0.344**
	2.177	0.295	−0.127						8	0.1	0.126	0.345
	1.987	0.337	0.137		×				9	1.017	0.127	0.348
	2.044	0.297		0.052					8	1.773	0.123	0.343
log(C$_{SD}$)	−0.805	0.08	−0.037						8	0	0.093	0.745
	−0.831	**0.08**							**7**	**0.632**	**0.092**	**0.743**
	−0.838	0.089	0.009		×				9	0.989	0.093	0.744
	−0.848	0.079		0.03					8	1.067	0.093	0.744
	−0.82	0.08	−0.03	0.019					9	1.543	0.093	0.745
sqrt(N$_{SD}$)	**0.308**	**0.02**							**7**	**0**	**0.145**	**0.416**
	0.304	0.02		0.007					8	0.55	0.147	0.415
	0.313	0.019	−0.005						8	0.924	0.146	0.414
	0.312	0.018		−0.007		×			9	1.947	0.148	0.418
Mg$_{SD}$	0.469	0.033	−0.059	−0.023	×				10	0	0.048	0.789
	0.44	0.042	−0.018	−0.023					9	1.055	0.046	0.79
	0.424	0.042		−0.017					8	1.255	0.046	0.788
	0.415	**0.041**							**7**	**1.294**	**0.045**	**0.787**
	0.451	0.033	−0.051		×				9	1.57	0.046	0.788
	0.474	0.033	−0.064	−0.031	×		×		11	1.935	0.048	0.789
sqrt(K$_{SD}$)	0.544	0.09	0.152	0.299	×	×	×	×	13	0	0.124	0.549
	0.699	0.057		0.098	×				9	0.75	0.116	0.533
	0.717	0.057	−0.021	0.092	×				10	0.758	0.118	0.537
	0.761	**0.044**							**7**	**1.65**	**0.11**	**0.531**
	0.7	0.056	0.00	0.116	×		×		11	1.755	0.118	0.538
	0.776	0.043	−0.019						8	1.777	0.111	0.535
sqrt(Ca$_{SD}$)	**1.003**	**0.049**	**−0.029**						**8**	**0**	**0.155**	**0.427**
	1.013	0.049	−0.033	−0.012					9	1.352	0.156	0.428
log(P$_{SD}$)	**−2.468**	**0.094**							**7**	**0**	**0.055**	**0.853**
	−2.486	0.094		0.032					8	0.252	0.056	0.852
	−2.455	0.094	−0.015						8	1.588	0.056	0.852

The simplest model for each trait according to the parsimony principle is highlighted in bold. For each model, information about the estimates of all the included explanatory variables, degrees of freedom, delta of Akaike information criterion (AIC), and marginal and conditional R^2 are provided. '×' indicates that the interaction term was included in the model. See Supporting Information Fig. S5 for more details in the effect sizes of the variables included in the competing models. df, degrees of freedom for the model; Int, intercept; PI_{ind}, individual phenotypic integration; R^2_m, marginal R^2; R^2_c, conditional R^2; S, Shannon diversity of the local neighborhood; TSP_{Div}, tree-species pair diversity.

2021) and intraspecific trait variation (Carvalho *et al.*, 2020; He *et al.*, 2021). However, at the within-individual level of biological organization used here, most metrics of trait variation showed an increase with PI_{ind}. Therefore, far from representing a constraint, PI_{ind} seems to be coupled with variation within an individual. Our results suggest that there is a link between the need of individuals to express alternative leaf designs and the maximization of the trait–trait coordination. As stated by Armbruster *et al.* (2014) and Zimmermann *et al.* (2016), phenotypic integration could act

as a facilitator of adaptation by reducing maladaptive uncoordinated variation. Indeed, this could be a strategy that would allow individuals to maximize their fitness while adjusting to heterogenous microenvironmental conditions within the canopy. However, even though the general patterns observed point out an increase in WTV with increasing PI_{ind}, the use of two complementary functional indices revealed that there are still intrinsic limits to trait variation (Valladares *et al.*, 2007; Auld *et al.*, 2010). While FDis was positively related to PI_{ind}, the total
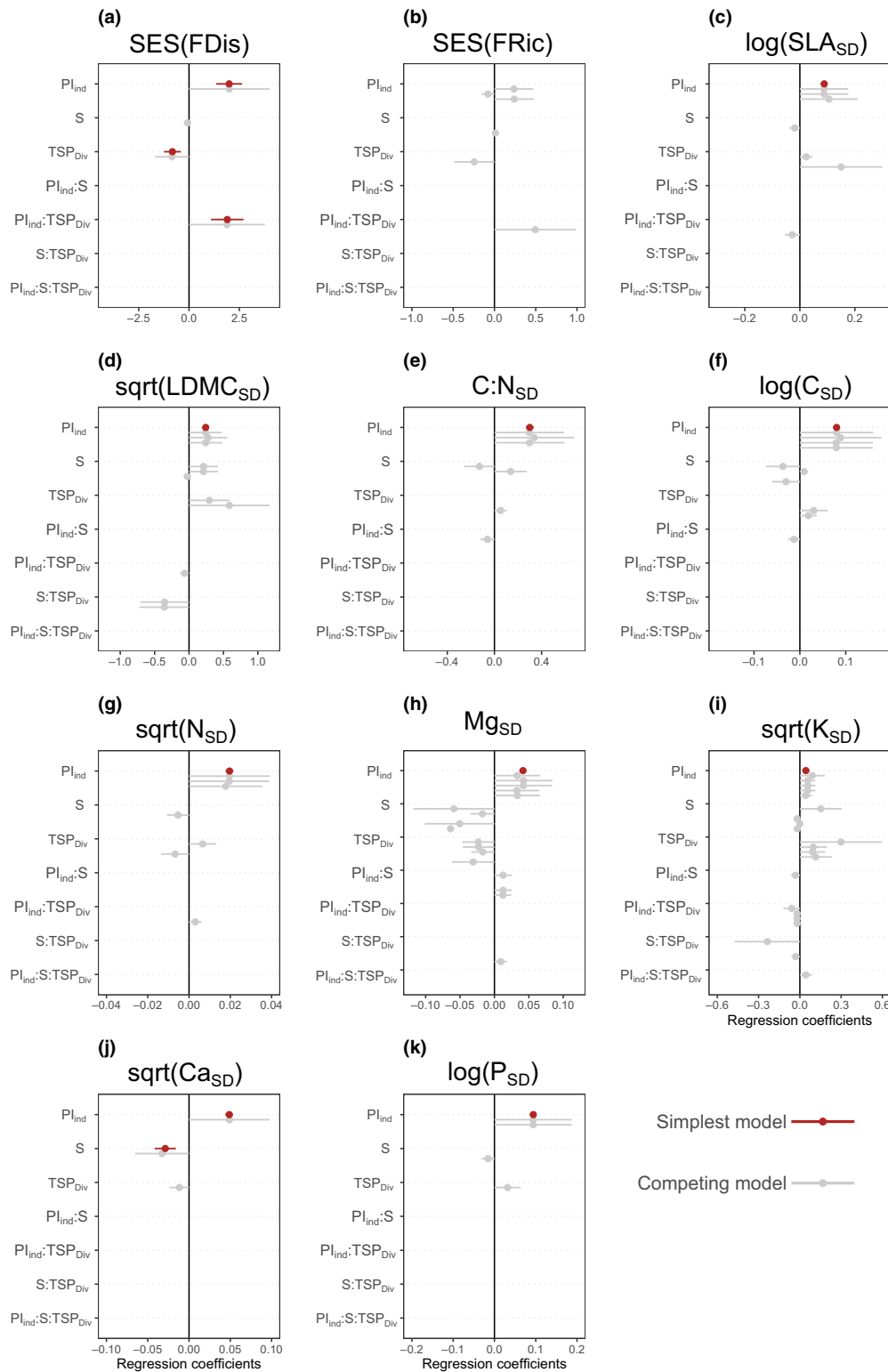
Fig. 3 Effects of the predictors in the simplest (red) and competing models (gray; ΔAICc < 2) for (a) the standarized effect size of functional dispersion (SES(FDis)) and (b) functional richness (SES(FRic)), and the standard deviation (SD) of (c) specific leaf area (SLA), (d) leaf dry matter content (LDMC), (e) carbon-to-nitrogen content (C : N), (f) leaf carbon content (c), (g) leaf nitrogen content (n), (h) leaf magnesium content (Mg), (i) leaf potassium content (K), (j) leaf calcium content (Ca), and (k) leaf phosphorous content (P), with 95% confidence intervals. Log and square-root transformations of the variables were indicated for every trait by log and sqrt, respectively. The acronyms correspond to the different predictors (PI_{ind}, individual phenotypic integration; S, Shannon diversity of the local neighborhood; TSPDiv, tree-species pair diversity), and interactions between predictors are indicated by ':'. For tree-species pairs, positive and negative coefficients indicate higher and lower values for conspecific tree-specific pairs compared with heterospecific tree-specific pairs, respectively. The lack of red error bars in (b) indicates that the simplest model for FRic did not include any predictor.
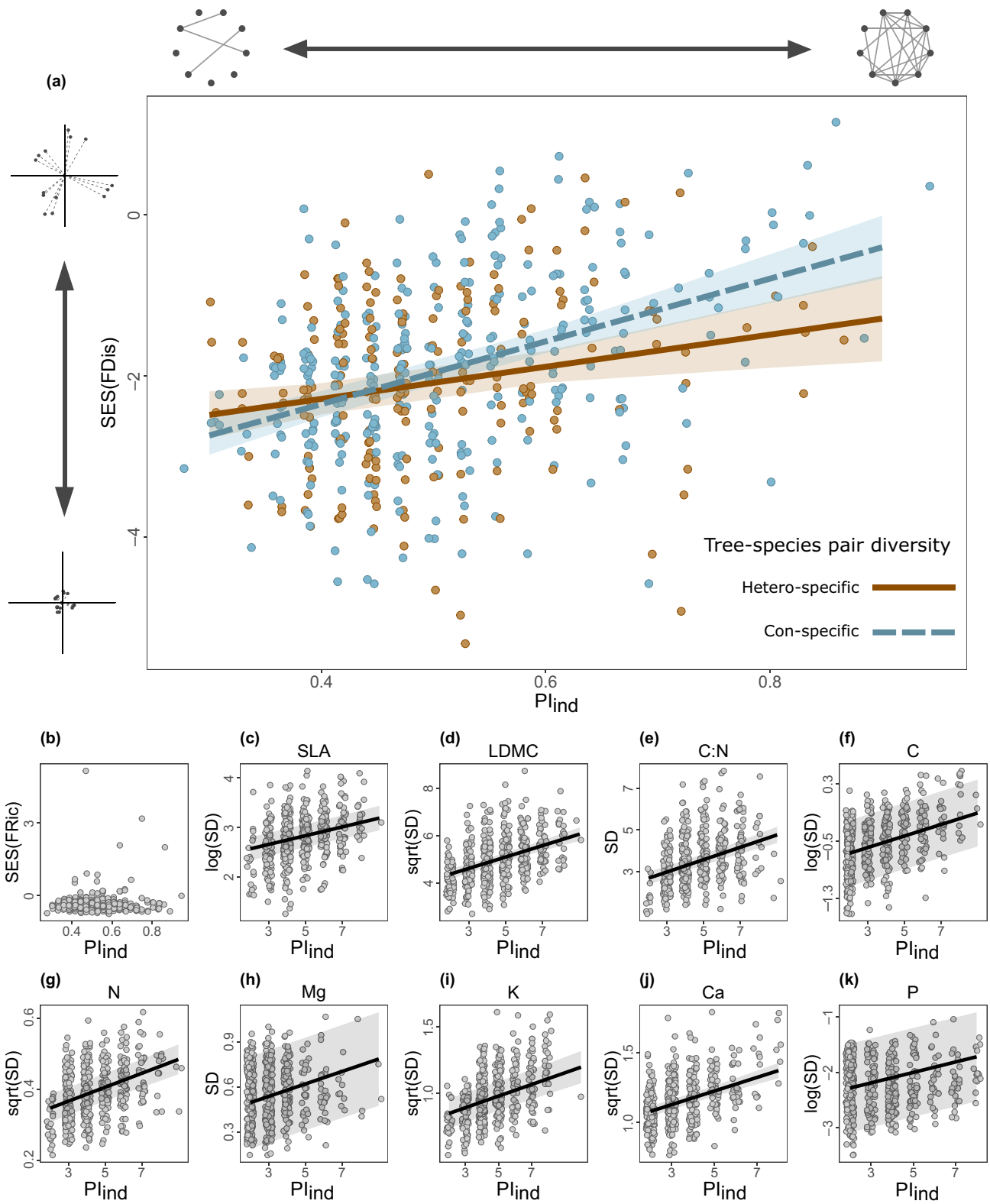
Fig. 4 Effects of PI_{ind} obtained in the simplest model according to the parsimony principle for (a) standardized effect size of functional dispersion (SES (FDis)), (b) standardized effect size of functional richness (SES(FRic)), (c) log-transformed standard deviation (SD) of specific leaf area (log(SLA_{SD})), (d) square-root-transformed SD of leaf dry matter content (sqrt($LDMC_{SD}$)), (e) SD of carbon-to-nitrogen ratio (($C : N)_{SD}$), (f) log-transformed SD of carbon leaf content (log(C_{SD})), (g) square-root-transformed SD of leaf nitrogen content (sqrt(N_{SD})), (h) SD of leaf magnesium content (Mg_{SD}), (i) square-root-transformed SD of leaf potassium content (sqrt(K_{SD})), (j) square-root-transformed SD of leaf calcium content (sqrt(Ca_{SD})), and (k) log-transformed SD of leaf phosphorous content (log(P_{SD})). Colored areas represent the confidence intervals at 95%. No effect was found for SES(FRic) in the simplest model (see Fig. 3; Table 2). Network diagrams on the upper panel illustrate the gradient from low to high PI_{ind}.
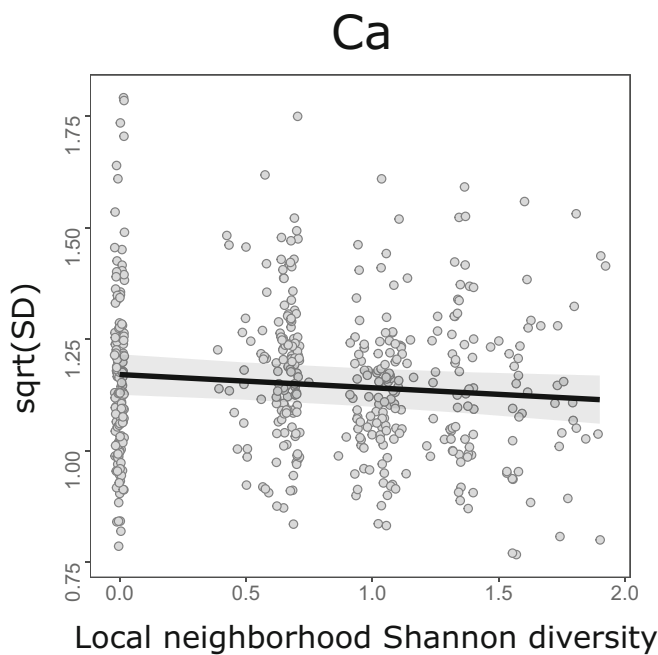
Ca

Fig. 5 Relationship between within-individual variation of leaf calcium (square-root transformed standard deviation (SD)) and Shannon diversity of the local neighborhood (see Table 2). Gray areas represent the confidence intervals at 95%.

it seems that even though the studied trees increase leaf diversity with PI_{ind}, trait variation is not unlimited (Valladares *et al.*, 2007).

Overall, we found weak effect of taxonomic diversity on WTV, suggesting that WTV could facilitate intraspecific plant–plant interactions by promoting slight niche complementarity. First, in the case of single traits, local neighborhood Shannon diversity reduced WTV of leaf Ca, and similar trends were found in at least one competing model for all other traits. Therefore, our results, even though are rather weak, suggest that trees may display higher WTV in monospecific communities. Indeed, this is consistent with similar patterns found for trees in a similar experiment in the tropics (Proß *et al.*, 2021). Second, the identity of the closest neighbor mediated the WTV-PI_{ind} relationship, as shown by the results for FDis, supporting that the positive effect of phenotypic integration on trait variation is stronger for trees with a conspecific closest neighbor. This result evidences that the role of phenotypic integration to prevent uncoordinated variation is even more important in the context of intraspecific competition. Thus, as higher WTV could facilitate intraspecific interactions by, for example, improving the efficiency of light capture (Møller *et al.*, 2022) and providing niche complementarity (Proß *et al.*, 2021), the steeper relationship with PI_{ind} in the presence of a conspecific may prevent maladjustment of leaf designs (Armbruster *et al.*, 2014). Considering these responses to taxonomic diversity and taking in account that WTV represents a great portion of the total trait diversity occurring within a species (Herrera *et al.*, 2015), we suggest that coexistence of individuals is not only driven by inter- and intraspecific trait variation. Rather, WTV could also constitute a mechanism that fosters niche complementarity.

Furthermore, the lack of strong responses of most single traits to taxonomic diversity (either heterospecificity of the closest neighbor or Shannon diversity of the local neighborhood) could

functional space filled by the individual (represented by FRic; Cornwell *et al.*, 2006) tended to remain unaffected by PI_{ind}. Thus, our results suggest that instead of occupying a larger niche volume, individual trees with higher PI_{ind} fill a similar trait space, but there are differences in the density and distribution of individual leaves within this trait space (Fig. 6). Leaves tend to be located in the inner part of the trait hypervolume when PI_{ind} is low and move toward the extremes as PI_{ind} increases. As a result,
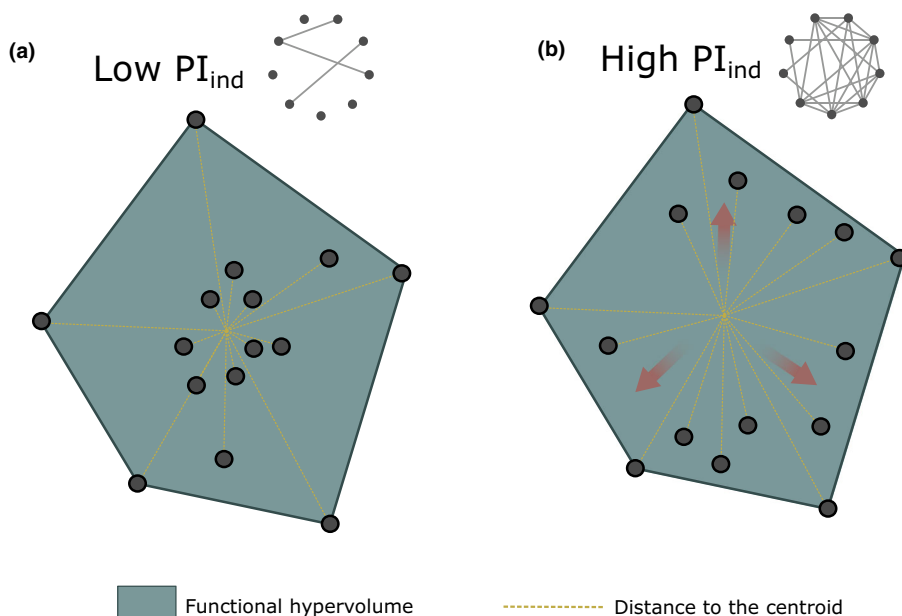

Fig. 6 Conceptual representation of the occupancy of the functional trait space under scenarios of (a) low and (b) high individual phenotypic integration (PI_{ind}), as suggested by our results. While overall trait space does not change, leaves (black points) tend to increase their distance to the centroid with higher PI_{ind}. Red arrows in (b) indicate the direction of the change detected by functional dispersion. Network diagrams illustrate scenarios of low and high PI_{ind}.

have two complementary explanations: as drivers of trait variation act on multiple traits simultaneously, multitrait approaches reflect variation patterns better than single-trait analyses (Albert *et al.*, 2010); and the relationship between WTV and taxonomic diversity could be hampered by other important drivers of WTV such as plant–animal interactions, and environmental factors like resource availability and climate predictability. Regarding plant–animal interactions, there is a growing literature showing the effect of pollination and seed dispersal on WTV of reproductive traits (Sobral *et al.*, 2010, 2019) and, specifically for the case of leaves, antagonistic interactions such as leaf herbivory have been suggested to select for higher WTV (Herrera, 2017). Concerning resource availability, Davrinche *et al.* (2023) showed that the relationship between WTV in leaves and diversity was dependent on the availability of nutrients in the soil. Last, higher WTV has been proposed to be an adaptive strategy to cope with unpredictability in rain regimes (March-Salas *et al.*, 2021).

While the variance explained by the predictors was not large, a large proportion of the variance in our data was attributed to random effects, including species identity and the location of the tree within the experiment. Species identity explains differences in trait variation (Mudrák *et al.*, 2019), supporting that species differing in their evolutionary history and adaptations exhibit differences in their plastic responses (Schlichting, 1986; Davidson *et al.*, 2011). Furthermore, because of its large spatial extent, the BEF-China experiment comprises environmental heterogeneity concerning, for example, slope, soil nutrients, and erosion (Scholten *et al.*, 2017), and it already has been observed that these differences influence intraspecific variation in the trees' crown shape (Perles-Garcia *et al.*, 2022). Indeed, as WTV also changes in response to small differences in abiotic conditions within the same habitat (Sobral *et al.*, 2019), it seems that differences in WTV among individuals could also be explained by their location within the experiment.

Concluding remarks

We aimed to provide new insights into the functional constraints of WTV, which, even though it is still widely understudied, seems to play a role in ecological processes (Sobral & Sampedro, 2022) and could be key for plants to adaptively respond to future scenarios of global change (March-Salas *et al.*, 2021). Although WTV is not unlimited, our study supports that integrated phenotypes maintain dissimilar leaf designs within the organism. This means that high PI_{ind} is needed to express large WTV and, as shown by our results, this is particularly important in the case of intraspecific interactions, where WTV could act as a stabilizing mechanism. Furthermore, if we aim to better understand WTV and its adaptive role for plants/trees in the response to future environmental conditions (Nicotra *et al.*, 2010), it should acknowledge that PI_{ind} also responds to abiotic factors (García-Verdugo *et al.*, 2009) and, therefore, following research on WTV and its limits should consider not only the WTV-PI_{ind} relationship but also its changes across environmental conditions.

Competing interests

None declared.

Author contributions

PCS-B, SH, SM and WSH conceived the idea and developed the methodology; under the supervision of SH, AD was responsible for leaf sample collection, laboratory analyses and trait predictions with Vis-NIRS, and PCS-B performed the statistical data analysis; PCS-B led the writing of the manuscript, with support from SH and SM. All the authors contributed to the reviewing and editing of the manuscript.

ORCID

Pablo Castro Sánchez-Bermejo https://orcid.org/0000-0003-3357-2980
Andréa Davrinche https://orcid.org/0000-0003-0339-2997
Sylvia Haider https://orcid.org/0000-0002-2966-0534
W. Stanley Harpole https://orcid.org/0000-0002-3404-9174
Silvia Matesanz https://orcid.org/0000-0003-0060-6136

Data availability

Code and data for the data analysis of this study are available at the Zenodo repository: doi: 10.5281/zenodo.8243092.

References

Aggarwal R, Ranganathan P. 2016. Common pitfalls in statistical analysis: the use of correlation techniques. *Perspectives in Clinical Research* 7: 187.

Albert CH, Thuiller W, Yoccoz NG, Douzet R, Aubert S, Lavorel S. 2010. A multi-trait approach reveals the structure and the relative importance of intra- vs interspecific variability in plant traits. *Functional Ecology* 24: 1192–1201.

Armbruster WS, Pélabon C, Bolstad GH, Hansen TF. 2014. Integrated phenotypes: understanding trait covariation in plants and animals. *Philosophical Transactions of the Royal Society of London. Series B: Biological Sciences* 369: 20130245.

Auld JR, Agrawal AA, Relyea RA. 2010. Re-evaluating the costs and limits of adaptive phenotypic plasticity. *Proceedings of the Royal Society B: Biological Sciences* 277: 503–511.

Barnes RJ, Dhanoa MS, Lister SJ. 1989. Standard normal variate transformation and de-trending of near-infrared diffuse reflectance spectra. *Applied Spectroscopy* 43: 772–777.

de Bello F, Lavorel S, Albert CH, Thuiller W, Grigulis K, Dolezal J, Janeček Š, Lepš J. 2011. Quantifying the relevance of intraspecific trait variability for functional diversity. *Methods in Ecology and Evolution* 2: 163–174.

Benavides R, Carvalho B, Matesanz S, Bastias CC, Cavers S, Escudero A, Fonti P, Martínez-Sancho E, Valladares F. 2021. Phenotypes of *Pinus sylvestris* are more coordinated under local harsher conditions across Europe. *Journal of Ecology* 109: 2580–2596.

Bolnick DI, Amarasekare P, Araújo MS, Bürger R, Levine JM, Novak M, Rudolf VHW, Schreiber SJ, Urban MC, Vasseur DA. 2011. Why intraspecific trait variation matters in community ecology. *Trends in Ecology & Evolution* 26: 183–192.

Botta-Dukát Z, Czúcz B. 2016. Testing the ability of functional diversity indices to detect trait convergence and divergence using individual-based simulation. *Methods in Ecology and Evolution* 7: 114–126.

Bruelheide H, Böhnke M, Both S, Fang T, Assmann T, Baruffol M, Bauhus J, Buscot F, Chen XY, Ding BY et al. 2011. Community assembly during secondary forest succession in a Chinese subtropical forest. *Ecological Monographs* 81: 25–41.

Bruelheide H, Nadrowski K, Assmann T, Bauhus J, Both S, Buscot F, Chen XY, Ding B, Durka W, Erfmeier A et al. 2014. Designing forest biodiversity experiments: general considerations illustrated by a new large experiment in subtropical China. *Methods in Ecology and Evolution* 5: 74–89.

Burnett AC, Anderson J, Davidson KJ, Ely KS, Lamour J, Li Q, Morrison BD, Yang D, Rogers A, Serbin SP. 2021. A best-practice guide to predicting plant traits from leaf-level hyperspectral data using partial least squares regression. *Journal of Experimental Botany* 72: 6175–6189.

Burnham KP, Anderson DR. 2004. *Multimodel inference: a practical information-theoretic approach.* New York, NY, USA: Springer.

Cabal C, Valladares F, Martinez-Garcia R. 2021. The ecology of plant interactions: a giant with feet of clay. *Preprints.* doi: 10.20944/ preprints202009.0520.v2.

Carvalho B, Bastias CC, Escudero A, Valladares F, Benavides R. 2020. Intraspecific perspective of phenotypic coordination of functional traits in Scots pine. *PLoS ONE* 15: 1–15.

Chase JM. 2014. Spatial scale resolves the niche vs neutral theory debate. *Journal of Vegetation Science* 25: 319–322.

Cornwell WK, Schwilk DW, Ackerly DD. 2006. A trait-based test for habitat filtering: convex hull volume. *Ecology* 87: 1465–1471.

Csardi G. 2021. *Package 'IGRAPH' R topics documented.* [WWW document] URL https://r.igraph.org/ [accessed 25 November 2021].

Davidson AM, Jennions M, Nicotra AB. 2011. Do invasive species show higher phenotypic plasticity than native species and, if so, is it adaptive? A meta-analysis. *Ecology Letters* 14: 419–431.

Davrinche A, Bittner A, Bruelheide H, Albert G, Harpole WS. 2023. High within-tree leaf trait variation and its response to species diversity and soil nutrients. *bioRxiv.* doi: 10.1101/2023.03.08.531739.

Davrinche A, Haider S. 2021. Intra-specific leaf trait responses to species richness at two different local scales. *Basic and Applied Ecology* 55: 20–32.

Dayal BS, Macgregor JF. 1997. Improved PLS algorithms. *Journal of Chemometrics* 11: 73–85.

De Kroon H, Huber H, Stuefer JF, Van Groenendael JM. 2005. A modular concept of phenotypic plasticity in plants. *New Phytologist* 166: 73–82.

Des Roches S, Post DM, Turley NE, Bailey JK, Hendry AP, Kinnison MT, Schweitzer JA, Palkovacs EP. 2018. The ecological importance of intraspecific variation. *Nature Ecology & Evolution* 2: 57–64.

Díaz S, Kattge J, Cornelissen JHC, Wright IJ, Lavorel S, Dray S, Reu B, Kleyer M, Wirth C, Colin Prentice I et al. 2016. The global spectrum of plant form and function. *Nature* 529: 167–171.

Dwyer JM, Laughlin DC. 2017. Constraints on trait combinations explain climatic drivers of biodiversity: the importance of trait covariance in community assembly. *Ecology Letters* 20: 872–882.

Escribano-Rocafort AG, Ventre-Lespiaucq AB, Granado-Yela C, Rubio De Casas R, Delgado JA, Balaguer L. 2016. The expression of light-related leaf functional traits depends on the location of individual leaves within the crown of isolated *Olea europaea* trees. *Annals of Botany* 117: 643–651.

Escribano-Rocafort AG, Ventre-Lespiaucq AB, Granado-Yela C, Rubio de Casas R, Delgado JA, Escudero A, Balaguer L. 2017. Intraindividual variation in light-related functional traits: magnitude and structure of leaf trait variability across global scales in *Olea europaea* trees. *Trees* 31: 1505–1517.

Escudero A, Matesanz S, Pescador DS, de la Cruz M, Valladares F, Cavieres LA. 2021. Every little helps: the functional role of individuals in assembling any plant community, from the richest to monospecific ones. *Journal of Vegetation Science* 32: e13059.

Escudero A, Valladares F. 2016. Trait-based plant ecology: moving towards a unifying species coexistence theory. *Oecologia* 180: 919–922.

Foley WJ, McIlwee A, Lawler I, Aragones L, Woolnough AP, Berding N. 1998. Ecological applications of near infrared reflectance spectroscopy – a tool for rapid, cost-effective prediction of the composition of plant and animal tissues and aspects of animal performance. *Oecologia* 116: 293–305.

García-Verdugo C, Granado-Yela C, Manrique E, de Casas RR, Balaguer L. 2009. Phenotypic plasticity and integration across the canopy of *Olea europaea* subsp. *guanchica* (Oleaceae) in populations with different wind exposures. *American Journal of Botany* 96: 1454–1461.

Garrenstjmuedu MSTG. 2019. *Package 'JMUOUTLIER'.* [WWW document] URL https://cran.r-project.org/web/packages/jmuOutlier/index.html [accessed 25 November 2021].

Gianoli E, Palacio-López K. 2009. Phenotypic integration may constrain phenotypic plasticity in plants. *Oikos* 118: 1924–1928.

Gotelli NJ, McCabe DJ. 2002. Species co-occurrence: a meta-analysis of J. M. Diamond's assembly rules model. *Ecology* 83: 2091–2096.

Götzenberger L, de Bello F, Bråthen KA, Davison J, Dubuis A, Guisan A, Lepš J, Lindborg R, Moora M, Pärtel M et al. 2012. Ecological assembly rules in plant communities-approaches, patterns and prospects. *Biological Reviews* 87: 111–127.

Gould SJ, Lewontin RC. 1979. The spandrels of San Marco and the Panglossian paradigm: a critique of the adaptationist programme. *Proceedings of the Royal Society B: Biological Sciences* 205: 581–598.

Grime JP. 1973. Competitive exclusion in herbaceous vegetation. *Nature* 242: 344–347.

Gross N, Robson TM, Lavorel S, Albert C, Le Bagousse-Pinguet Y, Guillemin R. 2008. Plant response traits mediate the effects of subalpine grasslands on soil moisture. *New Phytologist* 180: 652–662.

Grueber CE, Nakagawa S, Laws RJ, Jamieson IG. 2011. Multimodel inference in ecology and evolution: challenges and solutions. *Journal of Evolutionary Biology* 24: 699–711.

Harrison XA, Donaldson L, Correa-Cano ME, Evans J, Fisher DN, Goodwin CED, Robinson BS, Hodgson DJ, Inger R. 2018. A brief introduction to mixed effects modelling and multi-model inference in ecology. *PeerJ* 2018: 1–32.

Hart SP, Schreiber SJ, Levine JM. 2016. How variation between individuals affects species coexistence. *Ecology Letters* 19: 825–838.

He D, Biswas SR, Xu MS, Yang TH, You WH, Yan ER. 2021. The importance of intraspecific trait variability in promoting functional niche dimensionality. *Ecography* 44: 380–390.

He N, Li Y, Liu C, Xu L, Li M, Zhang J, He J, Tang Z, Han X, Ye Q et al. 2020. Plant trait networks: improved resolution of the dimensionality of adaptation. *Trends in Ecology & Evolution* 35: 908–918.

Herrera CM. 2009. *Multiplicity in unity. Plant subindividual variation and interactions with animals.* Chicago, IL, USA: University of Chicago Press.

Herrera CM. 2017. The ecology of subindividual variability in plants: patterns, processes, and prospects. *Web Ecology* 17: 51–64.

Herrera CM, Medrano M, Bazaga P. 2015. Continuous within-plant variation as a source of intraspecific functional diversity: patterns, magnitude, and genetic correlates of leaf variability in *Helleborus foetidus* (Ranunculaceae). *American Journal of Botany* 102: 225–232.

Herrera CM, Medrano M, Bazaga P, Alonso C. 2022. Ecological significance of intraplant variation: epigenetic mosaicism in *Lavandula latifolia* plants predicts extant and transgenerational variability of fecundity-related traits. *Journal of Ecology* 110: 2555–2567.

Homeier J, Seeler T, Pierick K, Leuschner C. 2021. Leaf trait variation in species-rich tropical Andean forests. *Scientific Reports* 11: 1–11.

Huneman P. 2010. Assessing the prospects for a return of organisms in evolutionary biology. *History and Philosophy of the Life Sciences* 32: 341–371.

Kuznetsova A, Brockhoff PB, Christensen RHB. 2017. LMERTEST package: tests in linear mixed effects models. *Journal of Statistical Software* 82: 1–26.

Laliberte E, Legendre P. 2010. A distance-based framework for measuring functional diversity from multiple traits. *Ecology* **91**: 299–305.

Laliberté E, Legendre P, Shipley B. 2014. *Package 'FD'. Measuring functional diversity from multiple traits, and other tools for functional ecology.* [WWW document] URL https://cran.r-project.org/web/packages/FD/index.html [accessed 26 November 2021].

Laughlin DC, Lusk CH, Bellingham PJ, Burslem DFRP, Simpson AH, Kramer-Walter KR. 2017. Intraspecific trait variation can weaken interspecific trait correlations when assessing the whole-plant economic spectrum. *Ecology and Evolution* **7**: 8936–8949.

Laughlin DC, Messier J. 2015. Fitness of multidimensional phenotypes in dynamic adaptive landscapes. *Trends in Ecology & Evolution* **30**: 487–496.

Li Y, Liu C, Sack L, Xu L, Li M, Zhang J, He N. 2022. Leaf trait network architecture shifts with species – richness and climate across forests at continental scale. *Ecology Letters* **25**: 1442–1457.

March-Salas M, Fandos G, Fitze PS. 2021. Effects of intrinsic environmental predictability on intra-individual and intra-population variability of plant reproductive traits and eco-evolutionary consequences. *Annals of Botany* **127**: 413–423.

Mason NWH, De Bello F, Mouillot D, Pavoine S, Dray S. 2013. A guide for using functional diversity indices to reveal changes in assembly processes along ecological gradients. *Journal of Vegetation Science* **24**: 794–806.

Matesanz S, Blanco-Sánchez M, Ramos-Muñoz M, de la Cruz M, Benavides R, Escudero A. 2021. Phenotypic integration does not constrain phenotypic plasticity: differential plasticity of traits is associated to their integration across environments. *New Phytologist* **231**: 2359–2370.

Mediavilla S, Martín I, Babiano J, Escudero A. 2019. Foliar plasticity related to gradients of heat and drought stress across crown orientations in three Mediterranean *Quercus* species. *PLoS ONE* **14**: 1–17.

Messier J, McGill BJ, Enquist BJ, Lechowicz MJ. 2017. Trait variation and integration across scales: is the leaf economic spectrum present at local scales? *Ecography* **40**: 685–697.

Møller C, March-Salas M, Kuppler J, De Frenne P, Scheepens JF. 2022. Intra-individual variation in *Galium odoratum* is affected by experimental drought and shading. *Annals of Botany* **131**: 411–422.

Mudrák O, Doležal J, Vítová A, Lepš J. 2019. Variation in plant functional traits is best explained by the species identity: stability of trait-based species ranking across meadow management regimes. *Functional Ecology* **33**: 746–755.

Nicotra AB, Atkin OK, Bonser SP, Davidson AM, Finnegan EJ, Mathesius U, Poot P, Purugganan MD, Richards CL, Valladares F et al. 2010. Plant phenotypic plasticity in a changing climate. *Trends in Plant Science* **15**: 684–692.

Nielsen M, Papaj DR. 2022. Why study plasticity in multiple traits? New hypotheses for how phenotypically plastic traits interact during development and selection. *Evolution* **76**: 858–869.

Olson DM, Dinerstein E, Wikramanayake ED, Burgess ND, Powell GVN, Underwood EC, D'Amico JA, Itoua I, Strand HE, Morrison JC et al. 2001. Terrestrial ecoregions of the world: a new map of life on Earth. *Bioscience* **51**: 933–938.

Osnas JLD, Lichstein JW, Reich PB, Pacala SW. 2013. Global leaf trait relationships: mass, area, and the leaf economics spectrum. *Science* **340**: 741–744.

Pérez-Harguindeguy N, Díaz S, Garnier E, Lavorel S, Poorter H, Jaureguiberry P, Bret-Harte MS, Cornwell WK, Craine JM, Gurvich DE et al. 2013. New handbook for standardised measurement of plant functional traits worldwide. *Australian Journal of Botany* **61**: 167–234.

Perles-Garcia MD, Kunz M, Fichtner A, Meyer N, Härdtle W, von Oheimb G. 2022. Neighbourhood species richness reduces crown asymmetry of subtropical trees in sloping terrain. *Remote Sensing* **14**: 1441.

Pigliucci M. 2005. Evolution of phenotypic plasticity: where are we going now? *Trends in Ecology & Evolution* **20**: 481–486.

Poorter H, Lambers H, Evans JR. 2014. Trait correlation networks: a whole-plant perspective on the recently criticized leaf economic spectrum. *New Phytologist* **201**: 378–382.

Proß T, Bruelheide H, Potvin C, Sporbert M, Trogisch S, Haider S. 2021. Drivers of within-tree leaf trait variation in a tropical planted forest varying in tree species richness. *Basic and Applied Ecology* **50**: 203–216.

R Core Team. 2021. *R: A language and environment for statistical computing.* Vienna, Austria: R Foundation for Statistical Computing. [WWW document] URL https://www.R-project.org/ [accessed 25 November 2021].

Rees M. 1993. Trade-offs among dispersal strategies in British plants. *Nature* **366**: 150–152.

Richards SA, Whittingham MJ, Stephens PA. 2011. Model selection and model averaging in behavioural ecology: the utility of the IT-AIC framework. *Behavioral Ecology and Sociobiology* **65**: 77–89.

Sack L, Melcher PJ, Liu WH, Middleton E, Pardee T. 2006. How strong is intracanopy leaf plasticity in temperate deciduous trees? *American Journal of Botany* **93**: 829–839.

Schlichting C, Pigliucci M. 1998. *Phenotypic evolution: a reaction norm perspective.* Sunderland, MA, USA: Sinauer Associates.

Schlichting CD. 1986. The evolution of phenotypic plasticity in plants. *Annual Review of Ecology, Evolution, and Systematics* **62**: 475–488.

Scholten T, Goebes P, Kühn P, Seitz S, Assmann T, Bauhus J, Bruelheide H, Buscot F, Erfmeier A, Fischer M et al. 2017. On the combined effect of soil fertility and topography on tree growth in subtropical forest ecosystems—a study from SE China. *Journal of Plant Ecology* **10**: 111–127.

Shannon CE. 1948. A mathematical theory of communication. *The Bell System Technical Journal* **27**: 379–423.

Shipley B, De Bello F, Cornelissen JHC, Laliberté E, Laughlin DC, Reich PB. 2016. Reinforcing loose foundation stones in trait-based plant ecology. *Oecologia* **180**: 923–931.

Silva JLA, Souza AF, Vitória AP. 2021. Leaf trait integration mediates species richness variation in a species-rich neotropical forest domain. *Plant Ecology* **222**: 1183–1195.

Sobral M, Guitián J, Guitián P, Violle C, Larrinaga AR. 2019. Exploring sub-individual variability: role of ontogeny, abiotic environment and seed-dispersing birds. *Plant Biology* **21**: 688–694.

Sobral M, Larrinaga AR, Guitián J. 2010. Do seed-dispersing birds exert selection on optimal plant trait combinations? Correlated phenotypic selection on the fruit and seed size of hawthorn (*Crataegus monogyna*). *Evolutionary Ecology* **24**: 1277–1290.

Sobral M, Sampedro L. 2022. Phenotypic, epigenetic, and fitness diversity within plant genotypes. *Trends in Plant Science* **27**: 843–846.

Su Y, Guo Q, Hu T, Guan H, Jin S, An S, Chen X, Guo K, Hao Z, Hu Y et al. 2020. An updated vegetation map of China (1:1000000). *Science Bulletin* **65**: 1125–1136.

Tilman D, Kilham SS, Kilham P. 1982. Phytoplankton community ecology: the role of limiting nutrients. *Annual Review of Ecology and Systematics* **13**: 349–372.

Trogisch S, Liu X, Rutten G, Xue K, Bauhus J, Brose U, Bu W, Cesarz S, Chesters D, Connolly J et al. 2021. The significance of tree-tree interactions for forest ecosystem functioning. *Basic and Applied Ecology* **55**: 33–52.

Valladares F, Gianoli E, Gómez JM. 2007. Ecological limits to plant phenotypic plasticity. *New Phytologist* **176**: 749–763.

Valladares F, Laanisto L, Niinemets Ü, Zavala MA. 2016. Shedding light on shade: ecological perspectives of understorey plant life. *Plant Ecology and Diversity* **9**: 237–251.

Valladares F, Niinemets Ü. 2008. Shade tolerance, a key plant feature of complex nature and consequences. *Review of Ecology and Systematics* **39**: 237–257.

Vasseur F, Westgeest AJ, Vile D, Violle C. 2022. Solving the grand challenge of phenotypic integration: allometry across scales. *Genetica* **150**: 161–169.

Violle C, Enquist BJ, McGill BJ, Jiang L, Albert CH, Hulshof C, Jung V, Messier J. 2012. The return of the variance: intraspecific variability in community ecology. *Trends in Ecology & Evolution* **27**: 244–252.

Violle C, Navas ML, Vile D, Kazakou E, Fortunel C, Hummel I, Garnier E. 2007. Let the concept of trait be functional! *Oikos* **116**: 882–892.

Watkinson AR, White J. 1986. Some life-history consequences of modular construction in plants. *Philosophical Transactions of the Royal Society of London. Series B: Biological Sciences* **313**: 31–51.

Winn AA. 1996. Adaptation to fine-grained environmental variation: an analysis of within-individual leaf variation in an annual plant. *Evolution* **50**: 1111–1118.

Wright A, Schnitzer SA, Reich PB. 2014. Living close to your neighbors: the importance of both competition and facilitation in plant communities. *Ecology* **95**: 2213–2223.

Wright IJ, Reich PB, Westoby M, Ackerly DD, Baruch Z, Bongers F, Cavender-Bares J, Chapin T, Cornelissen JHC, Diemer M *et al.* **2004.** The worldwide leaf economics spectrum. *Nature* **428**: 821–827.

Xie J, Wang Z. 2022. Stomatal opening ratio mediates trait coordinating network adaptation to environmental gradients. *New Phytologist* **235**: 907–922.

Yang X, Bauhus J, Both S, Fang T, Härdtle W, Kröber W, Ma K, Nadrowski K, Pei K, Scherer-Lorenzen M *et al.* **2013.** Establishment success in a forest biodiversity and ecosystem functioning experiment in subtropical China (BEF-China). *European Journal of Forest Research* **132**: 593–606.

Zimmermann TG, Andrade ACS, Richardson DM. 2016. Experimental assessment of factors mediating the naturalization of a globally invasive tree on sandy coastal plains: a case study from Brazil. *AoB Plants* **8**: plw042.

Supporting Information

Additional Supporting Information may be found online in the Supporting Information section at the end of the article.

Fig. S1 Selection of suitable data for the study of trait variation and phenotypic integration on individual trees.

Fig. S2 Analytical framework used to obtain the metrics of phenotypic integration and trait variation for every tree.

Fig. S3 *P*-values for trait–trait correlations.

Fig. S4 Testing independency between metrics of trait variation and phenotypic integration.

Fig. S5 Effect plots for all competing models for SES(FDis).

Fig. S6 Effect plots for all competing models for SES(FRic).

Fig. S7 Effect plots for all competing models for specific leaf area.

Fig. S8 Effect plots for all competing models for leaf dry matter content.

Fig. S9 Effect plots for all competing models for C : N.

Fig. S10 Effect plots for all competing models for C.

Fig. S11 Effect plots for all competing models for N.

Fig. S12 Effect plots for all competing models for Mg.

Fig. S13 Effect plots for all competing models for K.

Fig. S14 Effect plots for all competing models for Ca.

Table S1 Leaf traits included in our study, their ecological function, and literature describing them.

Table S2 Number and percentage of scans and leaves excluded in the process of outlier removal for every trait in every site of the experiment.

Table S3 Species included in our study and number of individuals in both study sites included in the analyses.

Table S4 Number of plots, TSPs, and trees sampled across all richness levels in the BEF-China experiment included in the analyses.

Table S5 Structure of the linear mixed models to study the relationship between individual phenotypic integration and trait variation under different scenarios of local taxonomic diversity.

Please note: Wiley is not responsible for the content or functionality of any Supporting Information supplied by the authors. Any queries (other than missing material) should be directed to the *New Phytologist* Central Office.